Available online at www.sciencedirect.com
ScienceDirect
Polymer 48 (2007) 966–974
polymer
www.elsevier.com/locate/polymer

The effect of organic modifier of the clay on morphology and crystallization properties of PET nanocomposites

C.I.W. Calcagno [a,b], C.M. Mariani [c], S.R. Teixeira [d], R.S. Mauler [c,*]

[a] PGCIMAT/UFRGS, Av. Bento Gonçalves, 9500 91501-970 Porto Alegre, Brazil
[b] CEFET/RS, Sapucaia do Sul, Brazil
[c] IQ/UFRGS, Av. Bento Gonçalves, 9500, P.O. Box 15003, 91501-970 Porto Alegre, Brazil
[d] IF/UFRGS, Av. Bento Gonçalves, 9500, P.O. Box 15051, 91501-970 Porto Alegre, Brazil

Received 14 September 2006; received in revised form 20 December 2006; accepted 21 December 2006
Available online 4 January 2007

Abstract

PET nanocomposites were prepared using montmorillonite with different organic modifiers (Cloisite® 15A, 30B and 10A). TEM, WAXD and DSC were used for the characterization. Nanocomposites of intercalated and exfoliated morphologies were obtained, and an average maximum distance between the platelets was observed in the intercalated morphology. The clay nucleated the PET crystallization process, and the nucleating effect was higher when Cloisite 10A was used. This study allowed the evaluation of the characteristics of the organic modifiers' influence on the intercalation and exfoliation processes in PET. Tactoids were obtained when only apolar modifiers were present. It was observed that PET nanocomposites were intercalated and exfoliated when polar modifiers were present.

Keywords: Nanocomposite; PET; Crystallization

1. Introduction

Nanocomposites show extraordinary advantages in the mechanical, thermal, optical and physicochemical properties when compared to the pure polymer or the conventional composites (with micrometer particles) with the use of low filler content (usually <6%) [1,2]. These properties are attractive, which justifies their tendency to enlarge the market of several polymers. The automotive (protection bars), packaging (bottles and films) and building (tubes and cables) segments are already using polymer nanocomposites, demonstrating the application potential of these materials [3–5]. The current tendency is to broaden the use of these materials by the plastic processors.

Nanocomposites obtained using different polymer matrices have been studied, for example, polyamides – PA (nylon) [6,7] polypropylene – PP [8], polyethylene – PE [9], polystyrene – PS [10], thermoplastic polyurethane – TPU [11], ethylene–vinyl acetate copolymer – EVA [12], poly(butylene terephthalate) – PBT [13], and others. Poly(ethylene terephthalate) – PET – is an engineering polymer that has been considered a commodity because of the diversity of its applications, as in packaging and fiber production. Comparatively to other polymers, there are few studies related to PET nanocomposites. Some of these studies have been focused on the use of the modified clay in PET polymerization studies [14–18]. The extrusion method was also used in the preparation of PET nanocomposites, which contributed to their better mechanical, thermal and barrier properties when compared to the pure polymer [19–21].

Among the potential nanocomposite precursors, those based on layered silicates (e.g., montmorillonite – MMT) have been more widely investigated [1]. The phyllosilicates are naturally hydrophilic and, in order to increase their organophilic characteristics, the cations in the gallery can be exchanged by cationic modifiers (e.g., quaternary ammonium

* Corresponding author.
E-mail address: mauler@iq.ufrgs.br (R.S. Mauler).

0032-3861/$ - see front matter © 2007 Elsevier Ltd. All rights reserved.
doi:10.1016/j.polymer.2006.12.044

salt). The modified clay (or organoclay) tends to present better compatibility with organic polymers [1].

Melt intercalation is a method to obtain nanocomposites, and the intercalation is improved by the use of conventional processing [6,7,22–24]. The extrusion has proved to be effective in the exfoliation and dispersion of the layered silicate. The success of the exfoliation is associated with the presence of strong interactions between the clay and the polymer chain, in addition to the shear and appropriate residence time [25].

The mixture between the polymer and the clay, to form intercalated and/or exfoliated systems, has been studied using theoretical models tested experimentally, indicating that the process involves contributions of different nature [26–32]. For example, the confinement of the polymer into the clay layers contributes to decrease of the entropy of the system, as well as disfavours the intercalation process. On the other hand, the chemical structure of the polymer can maximize the polymer–clay interactions and the presence of the organic modifiers can reduce the attraction among the clay layers, favoring the intercalation process and exfoliation.

In order to obtain nanocomposites, it is important to understand the interactions among the different components (clay–clay, polymer–clay, modifier–clay, modifier–polymer, etc.) within the intercalation and exfoliation processes. The objective of this work is to prepare PET nanocomposites using different clays in order to evaluate the effect of clay organic modifier on the morphology and crystallization properties of the nanocomposites.

2. Experimental

2.1. Materials

PET (Rhopet S-80 – Rhodia Ster – Mossi and Ghisolfi Group) and MMT (Cloisite® Na, Cloisite® 15A, Cloisite® 30B and Cloisite® 10A – Southern Clay Products) were dried at 140 °C, under vacuum, for approximately 4 h. The Cloisite® Na+ is a natural montmorillonite. The Cloisite 15A, Cloisite 30B and Cloisite 10A are natural clays modified with organic cations (Fig. 1).

2.2. Melt processing

PET and MMT (2–4%) were processed in a twin screw extruder (Haake H-25, model Rheomex PTW 16/25, $L/D = 25$), using a temperature profile of 225–240 °C in the die. PET was extruded in the same conditions without the clay.

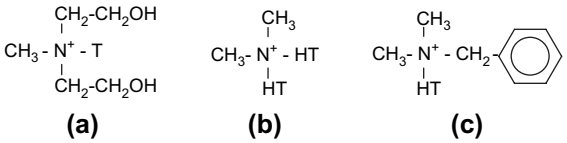

Fig. 1. Cationic modifiers on clays: (a) 30B; (b) 15A; (c) 10A. T = tallow = (~65% C18, ~30% C16, ~5% C14).

2.3. Films and specimens

Films and specimens were obtained by compression. The films were obtained by heating the polymer up to 260 °C, and maintained at this temperature for 5 min in order to obtain the complete melt of the pellets. After that, a pressure of 100 lbs was applied for 5 min. The sample was then cooled to room temperature at a cooling rate of ~20 °C/min. Similar conditions were used to obtain thicker specimens using decompression/compression for the elimination of air bubbles.

2.4. Wide angle X-ray diffraction (WAXD)

WAXD experiments were performed in a Siemens D-500 diffractometer. Films were scanned in the reflection mode using an incident X-ray of Cu Kα with wavelength of 1.54 Å at a step size of 0.05°/min from $2\theta = 1°$ to 10°.

2.5. Transmission electron microscopy (TEM)

The micrographs were carried out using ultrathin cuts obtained from the compressed specimens using a JEOL JEM-120 EXII TEM microscope operating at an accelerating voltage of 80 kV. The cuts were placed on 300 mesh Cu grids.

2.6. Differential scanning calorimetry (DSC)

Thermal and crystallization behaviors were determined using DSC Perkin–Elmer instruments. The temperature and energy readings were calibrated with indium and zinc according to ASTM D3417 and D3418. All measurements were carried out in nitrogen atmosphere. The sample was heated to 300 °C, held for 5 min at this temperature, then cooled and heated at constant rates of 10 °C/min.

2.7. Polarized optical microscopy (POM)

POM observation was performed using an Olympus-BX41 microscope using 40× lens. POM experiments were carried out by heating thin films to 250 °C and holding them for 5 min at this temperature. The crystallization was monitored during the cooling process.

2.8. ANOVA

Analysis of variance – ANOVA was used as a statistical method in order to evaluate the significance of T_c and T_m values considering a 95% confidence interval.

3. Results and discussion

3.1. Morphology of the nanocomposites

Four different clays were used and three of them are modified with ammonium salt. The space gallery was determined for the clays and PET nanocomposites using the Bragg law (Table 1). A decrease in the degree of coherent layer stacking

Table 1
WAXD and DSC data for PET and nanocomposites

	Basal distance[a] (Å)	T_m[b] (°C)	Clay (%)	T_c[b] (°C)	Crystallinity on cooling (%)	Crystallinity on heating (%)	Crystallization process ($\phi = 10$ °C/min)		
							$t_{1/2}$[c] (min)	Total time (min)	Temperature interval (°C)
PET	–	247	–	185	22 ± 3	22 ± 3	2.1	3.8	209–171
PETNa	–	250	2	198	31 ± 8	30 ± 9	1.6	3.7	216–162
PET10A	33.9	247	2	199	19 ± 3	18 ± 3.0	1.3	3.0	214–182
PET30B	33.9	247	2	193	30 ± 12	29 ± 13	1.8	4.7	213–165
			3	193	–	–	–	–	–
			4	193	–	–	–	–	–
PET15A	32.7	249	2	194	26 ± 8	26 ± 10	1.9	3.3	216–166
			3	195	–	–	–	–	–
			4	194	–	–	–	–	–

[a] Basal distance for pure clays are 12.8 Å in the MMTNa; 19.2 Å in the MMT10A; 18.8 Å in the MMT30B and 32.7 Å in the MMT15A.
[b] Standard deviation ± 1 °C.
[c] Standard deviation ± 0.2 min, except for PETNa and PET10A which was ±0.1 min.

(i.e. a more disordered system) of the clay would lead to peak broadening and a decrease of intensity in WAXD. The absence of the signal in WAXD suggests that the clay morphology is exfoliated when MMTNa was used (Fig. 2). When 30B and 10A clays were used, WAXD peak is shifted to lower angles, indicating the increase in interlayer spacing by the intercalation of polymer. For the PET15A, it was observed just as the narrowing of the characteristic clay peak and this indicates the presence of tactoids. In this sample the displacement of the peak at $2\theta = 6.9°$ was also observed, which is related to the existence of natural montmorillonite (MMTNa) even after the organic modification.

For all nanocomposites (except PETNa), the average maximum distance between the platelets was of about 33.9 Å. Above this distance, it is suggested that the platelets exfoliated. For clay–polymer mixtures, the intercalated or exfoliated morphology could be estimated by free energy consideration through the modelling of a mixture of long chain molecules and thin disks [29,30]. As the polymer diffuses through the energetically favorable gallery, it maximizes contact with the two confining silicate layers, and this results in a kinetically trapped state (the glue effect). The adhesive role of polymer chains between hydrophilic clay layers tends to strongly prohibit complete dissociation of clay nanoplatelets, usually resulting in only an intercalated state with a limited increase of gallery height [33]. Besides the appropriate choice of an organic modifier, when the nanocomposite is prepared in an extruder, the exfoliation process and dispersion of the layered silicate in the polymer matrix are influenced by the residence time and shear [6,7,34]. Paul and colleagues [6] demonstrated that the diffusion process has an important contribution to the delamination process. However, Lee and Kim [33] demonstrated that when the diffusion process is suppressed, it is possible to disperse the clay by shear application. In Fig. 3 it is possible to observe individual layers. It can be supposed that the shear in the extruder favours the exfoliation process, which results in both intercalated and exfoliated morphologies.

In TEM micrographs of the PET30B and PET15A, Fig. 3, it was possible to observe clay particles with a length of the 500 nm by 40 nm of thickness (or smaller), even under smaller magnifications. In the PET15A, longer and thicker particles are observed when compared to the PET30B. Although there are individual layers in the PET15A, they are present in a smaller amount. Several small dark points were observed in the PETNa micrographs (Fig. 4). In this sample, flat clay sheets are difficult to observe (Fig. 4b).

Micron sized clay particles are very rare. Only one particle present in the PET15A (Fig. 5) was possible to be visualized with its fragmentation in tactoids. Fornes and colleagues [7] suggested that, initially, the stress should help to break up large organoclay particles into dispersed stacks of silicate tactoids. In the extruder, the transfer of the stress from the molten polymer to the silicate tactoids is believed to shear them into smaller stacks of silicate platelets. Finally, individual platelets peel apart through a combination of shear and diffusion of polymer chains into the organoclay gallery. In the PET15A the formation of tactoids was observed, as in Fig. 5. However, the diffusion process occurs only in small amount.

Fig. 6 shows images obtained from different samples in which the clay layers appear to be able to bend, seeming quite flexible particles. Similar observations have been reported [6,7]. It is possible to suggest based on the TEM micrograph (Fig. 7) that the platelets peel apart and they roll up. The flexibility of the clay layers can explain the several small dark points observed mainly in the PETNa (Fig. 4), which may have the capability of rolling up after the exfoliation.

3.2. Thermal and crystallization behaviors

The T_c of the PET nanocomposites was higher than that of the pure PET. It can be supposed that this behavior is due to the presence of the clay (Table 1). Fig. 8 shows the crystallization curves of pure PET and nanocomposites. The higher T_c observed on the nanocomposites can be explained by the nucleation effect of the MMT on the PET. In this case, in the molten state, the segments of the PET molecules can easily interact with the surface of MMT, developing crystallization nuclei. Similar results have been reported for nanocomposites [9,35–37]. The values of T_c for PET30B and PET15A are

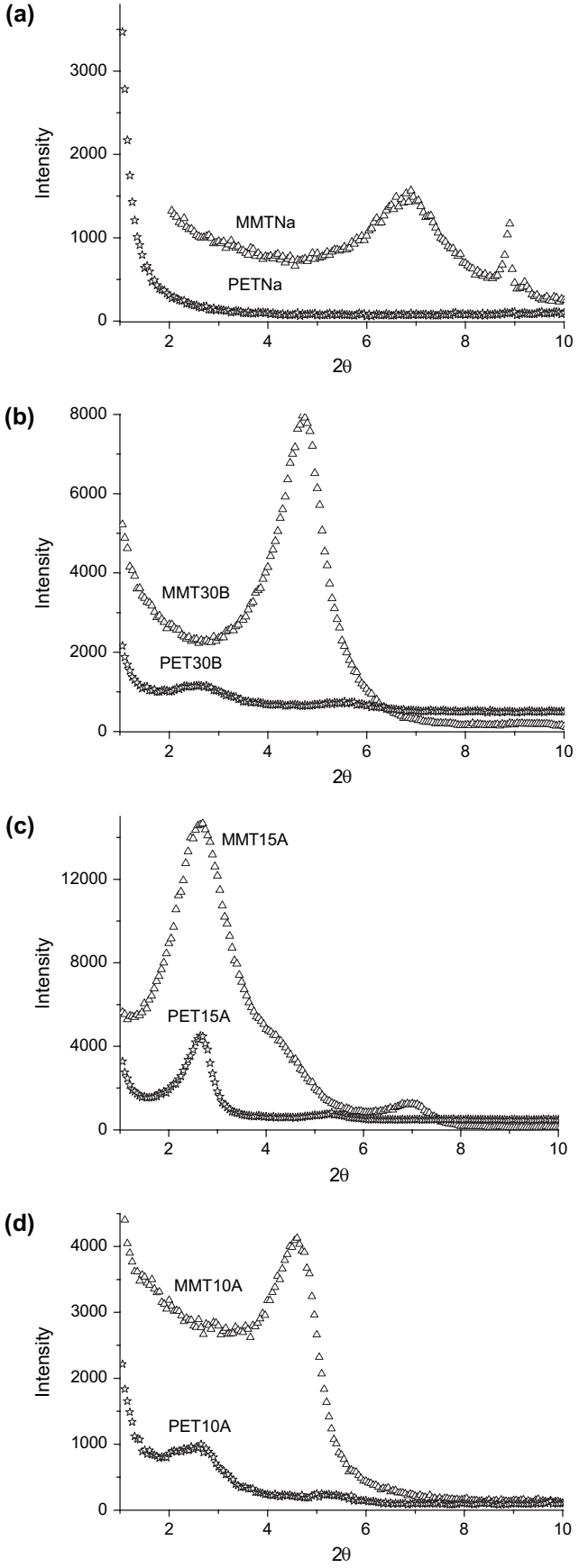

Fig. 2. Comparative WAXD: (a) MMTNa and PETNa; (b) MMT30B and PET30B; (c) MMT15A and PET15A; (d) MMT10A and PET10A.

similar. It was observed that the displacement in T_c was of about 4 °C higher for PET10A and PETNa. In these samples it is expected that a higher number of nuclei be formed as a consequence of the morphology of the clay. Although the PETNa was exfoliated, it has a smaller surface area available, and the T_c behavior is similar to that of PET10A. The samples with different amounts of clay showed similar morphology, and no significant variation was observed in the values of T_c (Table 1).

The total crystallinity of the nanocomposite values was slightly superior to that of the pure PET, as observed in Table 1. The higher dispersion of the values can be related to the heterogeneity of dispersion of the clay into the PET, resulting in different nucleating effects. The same crystallinity values in the cooling and in the heating processes indicate that, under those conditions, the crystallization process was complete during the cooling.

3.3. Non-isothermal crystallization

The development of relative degree of crystallinity (X_c) with the time (t) can be determined from non-isothermal process [9]. The total crystallization time is similar for PET and its nanocomposites, except for PET10A (Fig. 9 and Table 1). However, all nanocomposites reach the value of 95.0% of relative degree of crystallinity (Fig. 9b) more quickly than the pure polymer, indicating that the clay increases the crystallization rate of the PET. The decrease of the crystallization rate is observed in the final stage and can be explained by the collision of the crystals.

The $t_{1/2}$ value represents the necessary time for the system to reach 50% of relative degree of crystallinity, and it may be used to evaluate the rate of crystallization of different systems. Table 1 presents the $t_{1/2}$ values obtained at 10 °C/min. The $t_{1/2}$ values of nanocomposites were significantly smaller than those of the pure PET. Similar behavior has been reported in the literature [9,36]. The $t_{1/2}$ was not significantly affected by clay type, except when 10A clay was used, and this system presented smaller value.

The intervals of temperature to complete the crystallization of pure PET and nanocomposites are similar (Fig. 10). In the interval between 10 and 90% of relative degree of crystallinity, it is observed that the nanocomposites reach these percentiles at higher temperatures than pure PET. Besides, it is possible to verify that pure PET requests larger sub-cooling (larger temperature interval) to reach 10% of relative degree of crystallinity, which confirms the nucleating effect of the clay on the nanocomposite. The morphology of crystallization was observed by POM. It was possible to visualize a higher crystallization rate in the nanocomposites, and they present more nuclei and smaller spherulites' size than pure PET (Fig. 11).

3.4. Influence of the organic modifier on the nanocomposite morphology

There are entropic and enthalpic contributions in the clay/polymer mixture process to obtain intercalated and exfoliated

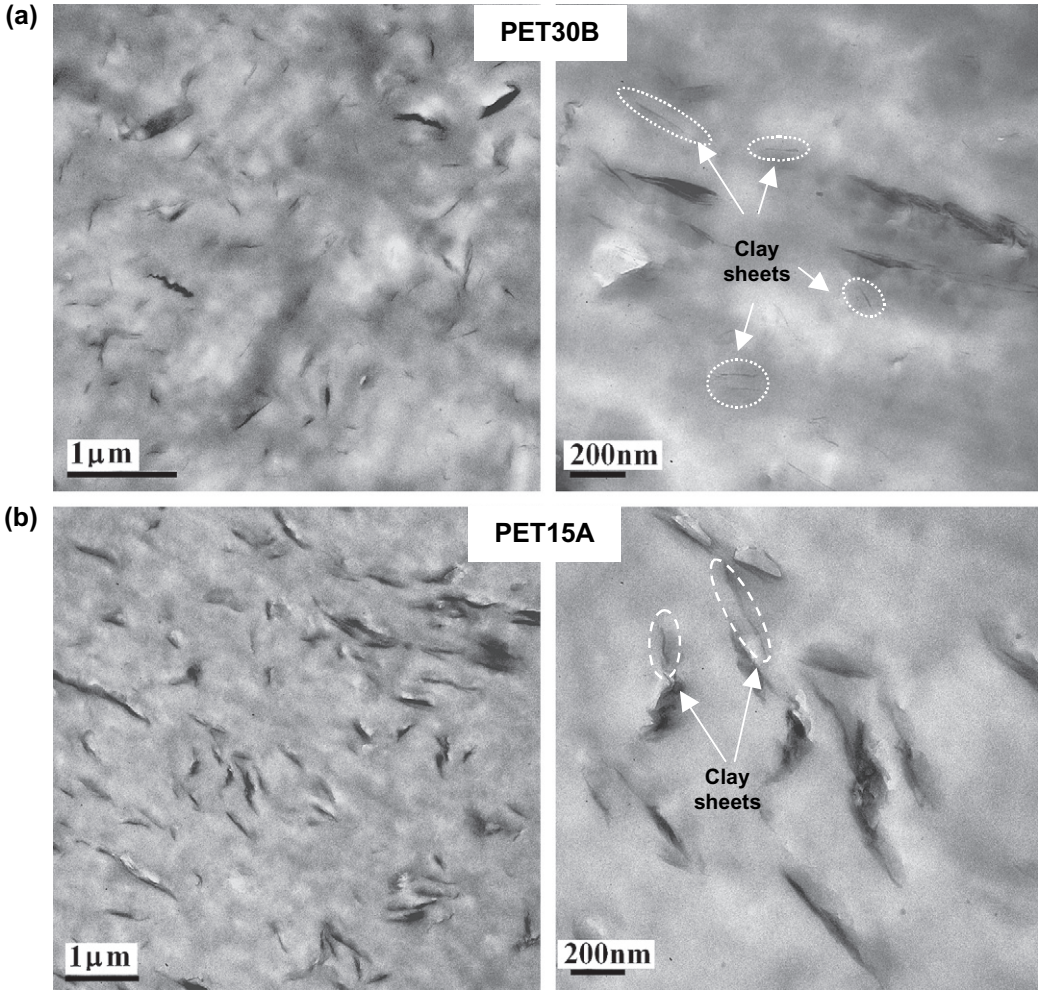

Fig. 3. Isolated clay sheets in TEM of the nanocomposites containing clays: (a) PET30B; (b) PET15A.

systems. The spacing between the closely packed sheets in MMT is of the order of 1 nm, increasing the entropic barrier associated with the penetration of the molten polymers into this gap [29]. One way to lower this entropic barrier is to use organically modified clays. For the appropriate choice of parameters, the energetic gains from the polymer–modifier interactions can outweigh the entropic losses. Under these conditions, the polymers can penetrate the gallery, separate the clay sheets, and potentially disperse the sheets within the melt [29]. Moreover, specific interactions between polymer and layered silicates at the interface were proposed to play an important role in changing the arrangement of intercalated molecules as well as the diffusion of molecules [33]. Exfoliated and homogeneous dispersions of the silicate layers can be obtained straightforwardly when the polymer contains functional groups, e.g., amide or imide groups [25]. A large amount of polar groups, such as the hydroxyl (OH) group that exists on the clay surface, is compatible with polymers containing polar functional groups and they are capable of strong intermolecular interaction [25]. Lee and Kim [33]

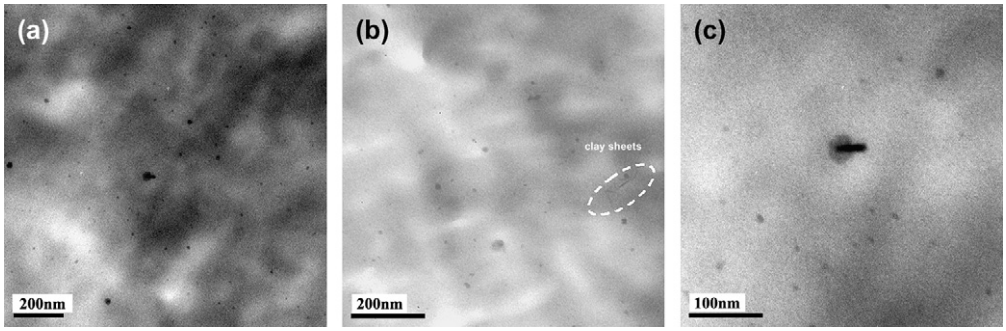

Fig. 4. TEM of the PETNa.

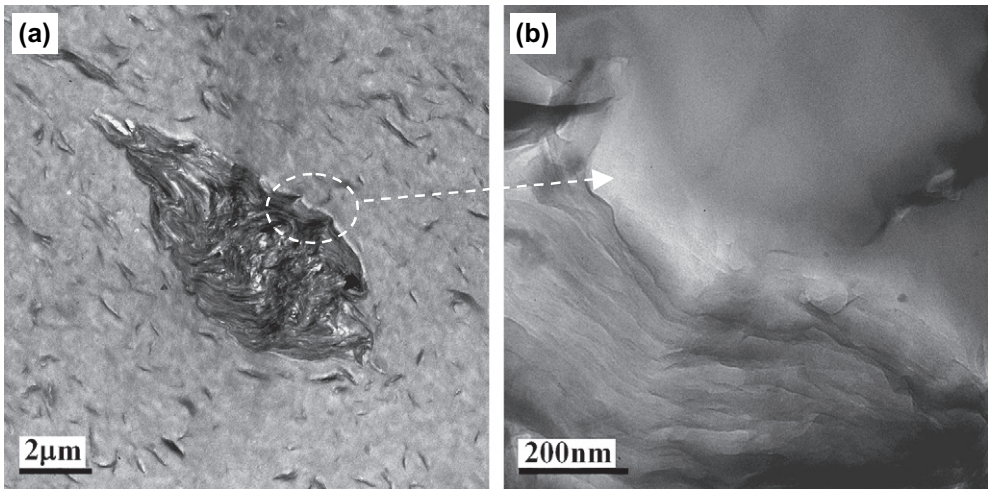

Fig. 5. Tactoids' fragmentation can be visualized on a micron sized particle in PET15A.

observed that the diffusion of the polymer was noticeably suppressed by the decrease of the polar interaction force in clay and it is inevitable to figure out the effect of hydrogen bonding on the polymer/clay intercalation behavior. Three different clay morphologies (tactoids, intercalated/exfoliated and exfoliated) were found in the PET nanocomposites when different clays were used under the same mixture conditions.

The intercalation of the polymer between the clay layers was not observed in PET15A. The cationic modifier in 15A clay (Fig. 1b) shows only apolar groups and two of them are long alkyl groups (dihydrogenated tallow). This system formed tactoids and a small amount of isolated sheets was observed. Besides the favorable PET–clay interactions, it can be mentioned the initial larger gallery spacing existent in this clay (32.7 Å) as favorable effect that would reduce the attraction between layers and it would aid the diffusion of the polymer chain into the gallery and increase the space. In PET15A, the unfavorable interaction among polar groups (of PET) and apolar groups (of the modifier) and the steric hindrance originated by the long alkyl groups superimpose the expected favorable effects. Similar results with nanocomposites of polar polymers have been reported [38–41].

The PET30B and PET10A nanocomposites showed both intercalated and exfoliated morphologies. The organic modifier of these clays (Fig. 1a and c) presents one long alkyl group and groups with relative polarity (bis-2-hydroxyethyl and benzyl, respectively). In these systems, the presence of just one long alkyl group reduces the number of unfavorable interactions between the polymer and the modifier, and a larger number of interactions between the clay and PET can occur. Moreover, there is a decrease in the number of unfavorable interactions between the clay and the long alkyl group. The polarity impute by the presence of the polar groups on the modifier can also favour the diffusion of the polymer into the gallery, originating intercalated morphology. These considerations can explain the best results of the 30B and 10A clays in comparison with the 15A clay in the formation of the exfoliated/intercalated morphology. Similar results have been reported for nylon-6 [38,39], poly(ethylene oxide) [41], poly(ethylene terephthalate-*co*-ethylene naphthalate [40] and

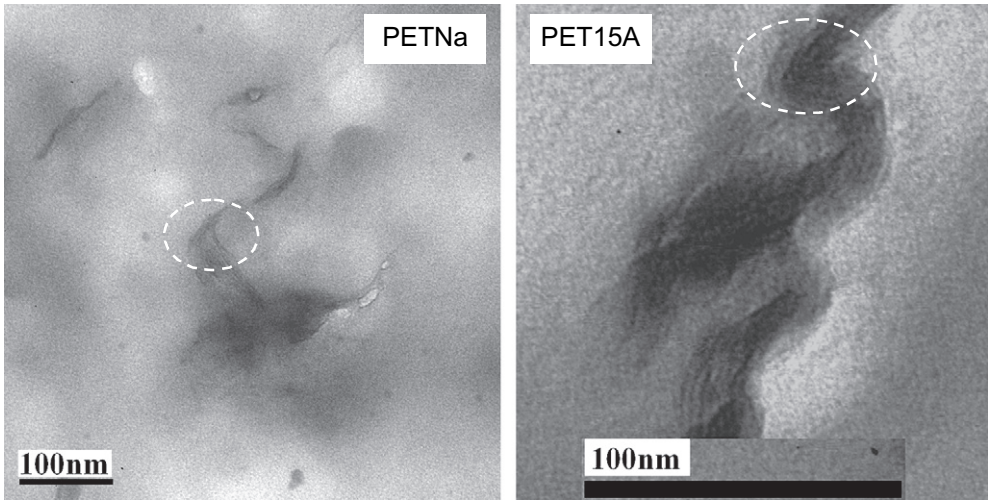

Fig. 6. Flexibility of the clay layers.

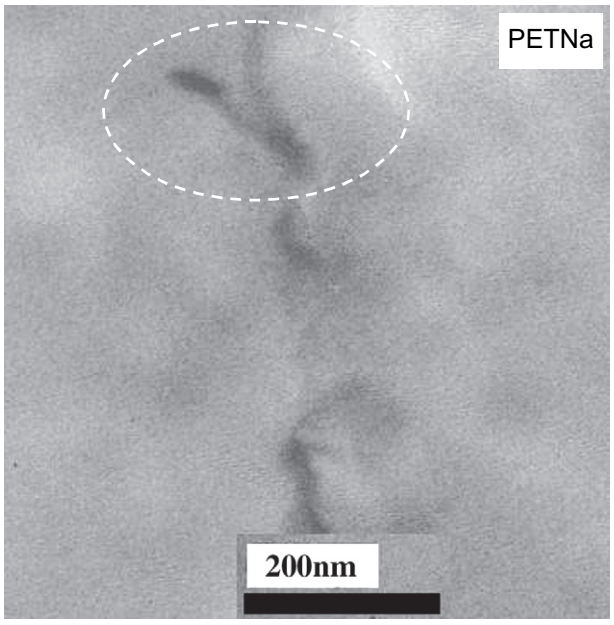

Fig. 7. Flexibility of the clay layers in the PETNa.

aliphatic polyester [42] nanocomposites. PET10A showed higher nucleating effect. This result can be related to the presence of the aromatic ring in the modifier as in the PET chain, that favours the diffusion process, resulting in more sheets of clay and, consequently more crystallization nuclei.

In the PETNa the organized clay arrangement was destroyed and small dark points were observed by TEM. Jang et al. [32] classified the PET as a polymer with a medium solubility parameter and, according to these authors, the intercalation and exfoliation of the clay in these systems are expected only if the organically modified clays were used. According to Vaia and Giannelis [26,27], immiscible, intercalated and delaminated morphologies were explained in terms of the free energy changes using the mean-field model, and it was suggested that the delaminated structures were obtained in systems with favorable polymer–clay interactions. In the PETNa the modifier was not present and it seems that the polymer–clay interactions and the extrusion (shear) conditions were sufficient to break the organized arrangement of the clay, dispersing the layers in the polymer matrix. It was also

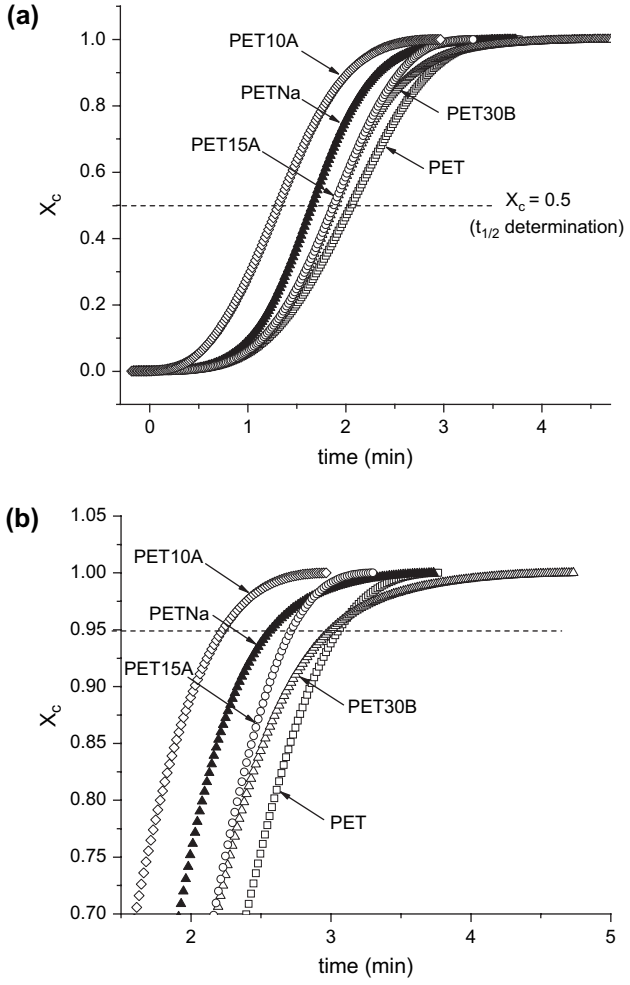

Fig. 9. Development of relative degree of crystallinity (X_c) with the time (t) at cooling rate = 10 °C/min: (a) total interval; (b) final stage.

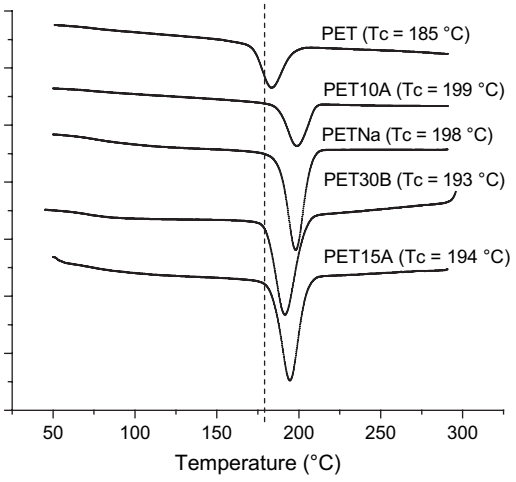

Fig. 8. Crystallization behavior of pure PET and nanocomposites (cooling rate = 10 °C/min).

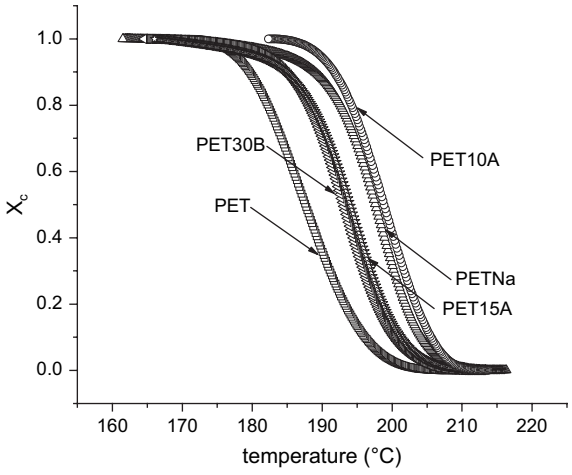

Fig. 10. Development of relative degree of crystallinity (X_c) with the temperature (T) at cooling rate = 10 °C/min.

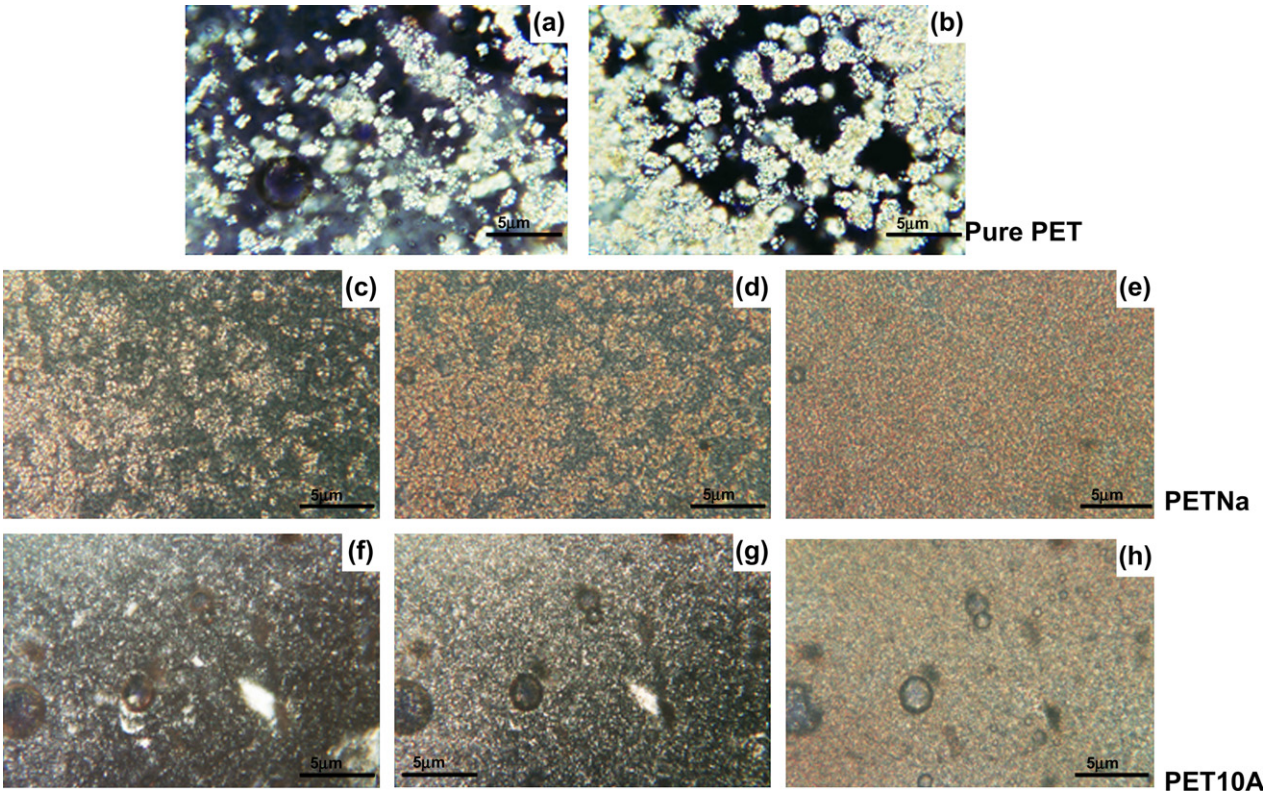

Fig. 11. POM crystallization sequence of: (a) the pure PET; (b) PETNa; (c) PET10A.

observed that the extrusion process fragments the clay into smaller particles (tactoids or intercalated clay) and/or individual platelets (Figs. 3, 4 and 6). Usually, the length of the exfoliated clay sheets is smaller than 100 nm. In the MMTNa the organic modifier is absent. Then it could assume that due to intramolecular interactions in the exfoliated clay sheet, and its flexibility, it may rolls up (Fig. 4c). In systems where samples were prepared by solutions this morphology was more frequently observed by TEM [43]. When organic modifier is present, it protects the clay surface, and hinders that exfoliated clay sheets to roll.

4. Conclusion

Intercalated and exfoliated PET nanocomposites were successfully prepared. An average maximum distance between the platelets was of about 33.9 Å for all intercalated nanocomposites. Above this distance, it was suggested that the platelets exfoliated. The shear in the extruder favours the exfoliation process, which results in both intercalated and exfoliated morphologies. The clay acts as nucleating agent and increases the crystallization rate of the PET. The nanocomposites present more nuclei and smaller spherulites' size than pure PET. PET nanocomposites using clay with polar modifiers showed intercalated and exfoliated morphologies and tactoids were obtained when only apolar modifiers were presented. The polymer–clay interactions and the extrusion conditions were sufficient to break the organized arrangement of the natural montmorillonite, dispersing it in the polymer matrix. The organic modifier seems to sustain the exfoliated clay sheets flat. In its absence the intramolecular interactions are stronger and the platelets may roll due to its high flexibility.

Acknowledgments

The authors gratefully acknowledge Conselho Nacional de Desenvolvimento Científico e Tecnológico – CNPq and Pronex/FAPERGS for financial support.

References

[1] Alexandre M, Dubois P. Mater Sci Eng 2000;28:1–63.
[2] Ray SS, Okamoto M. Prog Polym Sci 2003;28:1539–641.
[3] Plast Addit Compounding 2002;30–3.
[4] Gao F. Mater Today 2004;50–5.
[5] Pack 2005;96:20–1.
[6] Dennis HR, Hunter DL, Chang D, Kim S, White JL, Cho JW, et al. Polymer 2001;42:9513–22.
[7] Fornes TD, Yoon PJ, Keskkula H, Paul DR. Polymer 2001;42:9929–40.
[8] Manias E, Touny A, Wu L, Strawhecker K, Lu B, Chung TC. Chem Mater 2001;13:3516–23.
[9] Xu WB, Zhai HB, Guo HY, Zhou ZF, Whitely N, Pan W-P. J Therm Anal Calorim 2004;78:101–12.
[10] Sohn J-I, Lee CH, Lim ST, Kim TH, Choi HJ, Jhon MS. J Mater Sci 2003;38:1849–52.
[11] Chen-Yang YW, Yang HC, Li GJ, Li YK. J Polym Res 2004;11:275–83.
[12] Peeterbroeck S, Alexandre M, Jérôme R, Dubois P. Polym Degrad Stab 2005;90:288–94.
[13] Acierno D, Scarfato P, Amendola E, Nocerino G, Costa G. Polym Eng Sci 2004;44(6):1012–8.
[14] Zhang G, Shichi T, Takagi K. Mater Lett 2003;57:1858–62.

[15] Imai Y, Nishimura S, Abe E, Tateyama H, Abiko A, Yamaguchi A, et al. Chem Mater 2002;14:477–9.
[16] Saujanya C, Imai Y, Tateyama H. Polym Bull 2002;49:69–76.
[17] Di Lorenzo ML, Errico ME, Avella M. J Mater Sci 2002;37:2351–8.
[18] Ke Y-C, Yang Z-B, Zhu C-F. J Appl Polym Sci 2002;85:2677–91.
[19] Davis CH, Mathias LJ, Gilman JW, Schiraldi DA, Shields JR, Trulove P, et al. J Polym Sci Part B Polym Phys 2002;40:2661–6.
[20] Pegoretti A, Kolarik J, Peroni C, Migliaresi C. Polymer 2004;45:2751–9.
[21] Vidotti SE, Chinellato AC, Boesel LF, Pessan LA. J Metastable Nanocrys Mater 2004;22:57–64.
[22] Vaia RA, Jandt KD, Kramer EJ, Giannelis EP. Macromolecules 1995;28: 8080–5.
[23] Vaia RA, Jandt KD, Kramer EJ, Giannelis EP. Chem Mater 1996;8: 2628–35.
[24] Cho JW, Paul DR. Polymer 2001;42:1083–94.
[25] Sanchez-Solís A, Romero-Ibarra I, Estrada MR, Calderas F, Manero O. Polym Eng Sci 2004;44(6):1094–102.
[26] Vaia RA, Giannelis EP. Macromolecules 1997;30:7990–9.
[27] Vaia RA, Giannelis EP. Macromolecules 1997;30:8000–9.
[28] Vaia RA, Ishii H, Giannelis EP. Chem Mater 1993;5:1694–6.
[29] Balazs AC, Singh C, Zhulina E. Macromolecules 1998;31:8370–81.
[30] Lyatskaya Y, Balazs AC. Macromolecules 1998;31:6676–80.
[31] Zhulina E, Singh C, Balazs AC. Langmuir 1999;15:3935–43.
[32] Jang BN, Wang D, Wilkie CA. Macromolecules 2005;38:6533–43.
[33] Lee S-S, Kim JY. J Polym Sci Part B Polym Phys 2004;42(12):2367–72.
[34] Gopakumar TG, Lee JA, Kontopoulou M, Parent JS. Polymer 2002;43: 5483–91.
[35] Ou CF, Ho MT, Lin JR. J Polym Res 2003;10:127–32.
[36] Wang Y, Shen C, Li H, Li Q, Chen J. J Appl Polym Sci 2004;91:308–14.
[37] Wu Z, Zhou C, Zhu N. Polym Test 2002;23:479–83.
[38] Fornes TD, Hunter DL, Paul DR. Macromolecules 2004;37:1793–8.
[39] Fornes TD, Yoon PJ, Hunter DL, Keskkula H, Paul DR. Polymer 2002; 43:5915–33.
[40] Lai M, Kim J-K. Polymer 2005;46:4722–34.
[41] Loyens W, Jannasch P, Maurer FHJ. Polymer 2005;46:903–14.
[42] Lee S-R, Park H-M, Lim H, Li X, Cho W-C, Ha C-S. Polymer 2002;43: 2495–500.
[43] Unpublished results.